JGR Atmospheres

RESEARCH ARTICLE
10.1029/2019JD030895

Key Points:

- The technique of electric cloud structure estimation based on WRF simulation of a convective event is developed
- A dipole structure with a positive lower layer is typical for the thunderclouds producing intense thunderstorm ground enhancements (TGEs)
- Snow and graupel particles are the main charge carriers in the mountain conditions of TGE occurrence

Supporting Information:

Supporting Information may be found in the online version of this article.

Correspondence to:

E. K. Svechnikova,
svechnikova@ipfran.ru

Citation:

Svechnikova, E. K., Ilin, N. V., Mareev, E. A., & Chilingarian, A. A. (2021). Characteristic features of the clouds producing thunderstorm ground enhancements. *Journal of Geophysical Research: Atmospheres*, *126*, e2019JD030895. https://doi.org/10.1029/2019JD030895

Received 26 APR 2019
Accepted 1 APR 2021

Characteristic Features of the Clouds Producing Thunderstorm Ground Enhancements

E. K. Svechnikova[1,2], N. V. Ilin[1], E. A. Mareev[1,2], and A. A. Chilingarian[3]

[1]Institute of Applied Physics, Russian Academy of Sciences, Nizhny Novgorod, Russia, [2]Lobachevsky State University, Nizhny Novgorod, Russia, [3]A. Alikhanyan National Lab (Yerevan Physics Institute), Yerevan, Armenia

Abstract Thunderstorm ground enhancements (TGEs) are fluxes of energetic particles multiplied in thunderclouds, which may be registered by ground-based detectors. Using the Weather Research and Forecasting (WRF) Model, the state of the atmosphere with a 1-km horizontal resolution is modeled for convective events accompanied by TGEs observed at the high altitude Aragats Research Station in Armenia (40.47 N, 44.18 E, 3,200 m above sea level). By comparing the data obtained in observations with the results of simulations using a microphysical parameterization for WRF, a technique is developed for estimating charge distribution parameters. A typical charge distribution in a TGE-producing cloud is found to be well approximated by a two-layered charge structure with a lower positive charge region formed by graupel particles and an upper negative charge region formed by snow particles. The characteristic charge density is 0.01 nC/m^3 for the graupel cluster and −0.02 nC/m^3 for the snow cluster. A vertical distance of about 1–2 km between the lower positive and upper negative layers is sufficient for the development of an energetic particle avalanche.

1. Introduction

Studying high-energy phenomena in the Earth's atmosphere involves several aspects of climatology and atmospheric physics. The question of the mechanisms of energetic particle flux generation is directly related to the problem of lightning discharge initiation. Thunderstorm ground enhancement (TGE) (Chilingarian et al., 2010, 2013) is an excess of the electron and gamma-ray fluxes over background values (from tens to hundreds of percent) detected at the Earth's surface. TGE can include short-term (several minutes) and long-term (up to several hours) components of radiation. A long-term component is caused by the gamma radiation of the radon progeny and has energy below 3 MeV (Chilingarian, Hovsepyan, et al., 2019). It is generally agreed that a short-term gamma-emission of thunderclouds is caused by the bremsstrahlung of energetic "runaway" electrons. In the electric field of a thundercloud, electrons can accelerate via a runaway process (Gurevich et al., 1992) and experience multiplication forming avalanches of runaway electrons (Dwyer, 2003). The propagation of runaway electrons in the electric field of a thundercloud is accompanied by the production of the bremsstrahlung gamma radiation.

In 2016 and 2017, more than 200 TGE events were observed at the Aragats Research Station. This study describes eight TGE events that allow detailed consideration because of an especially large amount of gained data. Observational data on the fluxes of energetic particles from thunderclouds complement the information about the electrical properties of these clouds. New information on the structure of thunderclouds and the dynamics of the processes occurring in them, in turn, enriches the methods for predicting atmospheric phenomena, including lightning activity. On a time scale of tens of minutes, a cloud moves a few kilometers horizontally, making it possible to measure the electric field created by its different parts with stationary instruments. During this period, the charge dissipation does not play a major role in the evolution of the electrical structure (McGorman & Rust, 1998, p. 33; Stolzenburg et al., 2015).

Direct balloon measurements have not been carried out for the research of TGE-producing clouds in Aragats. Available data obtained by weather radars are insufficient to describe the distribution of cloud particles in the atmosphere (data on the maximum radar reflectivity are presented in Supporting Information). At the same time, numerical simulation of the state of the atmosphere, which has reached higher reliability due to its rapid development in the past two decades (Thorpe, 2013), is a valuable source of information on the cloud structure and has been successfully used in studies of atmospheric electricity phenomena

(Dementyeva et al., 2015; Lynn & Yair, 2010; Xu et al., 2016). In the present study, the electrical structure of a cloud is estimated using numerical modeling of the state of the atmosphere and the results of ground-based measurements of the electric field. Because of the nonuniqueness of a charge distribution capable of producing the electric field dynamics measured on the ground, several assumptions are made concerning the distribution of charge on cloud particles. The analysis performed in this study can be considered as an initial step on the way to a detailed investigation of the structure of TGE-producing clouds. If we see that the WRF model can reflect a "large-scale" structure reasonably well, we will be able to move toward smaller-scale simulations with radar data assimilation. Any cloud model with a higher resolution would require specifying initial and boundary conditions. The proposed modeling technique can provide these conditions for further simulations using a nested grid with a smaller scale.

In Sections 2 and 3, observational data and atmospheric modeling applied in this study are described. Section 4 describes the proposed technique of estimating the electrical structure of a cloud, based on a comparison of measurement results with numerical simulation performed by means of the Weather Research and Forecasting Model (the WRF model). Sections 5 and 6 contain the results of applying the technique to two intense TGE events (June 11, 2016 and June 21, 2017), including the inferred spatial distribution of hydrometeors (cloud particles) and charge distribution within a cloud. The estimated electrical structure is discussed in the context of the role of different hydrometeor types and the conditions of relativistic runaway electron avalanche generation.

2. Experimental Data Used for the Research

In the current study, we use the data on the surface electric field and energetic particle flux obtained at the Aragats Research Station, available at http://crd.yerphi.am/, a description of the Station can be found in Chilingarian et al. (2010). A 3-cm thick plastic scintillator of the Stand-3 detector is used to register gamma photons with an energy greater than 3 MeV. The scintillation detector has 99% efficiency for electrons and 3%–4% efficiency for gamma-photons (Chilingarian et al., 2010). The radiation of radon progenies has an upper limit of 3 MeV, therefore, the energy threshold of the Stand-3 detector ensures that measurements are not influenced by radon contamination (Chilingarian, Hovsepyan, et al., 2019). The electric field was measured by the Electric Field Monitor Boltek EFM-100, located 70 m from the energetic particle detector. The Boltek EFM-100 Electric Field Monitor measures the static electric field with an error of 10% in a range of field values up to 40 kV/m (EFM-100 Atmospheric Electric Field Monitor, 2016). Positive values of the electric field correspond to the downward direction in accordance with the atmospheric physics sign convention.

3. Atmospheric Modeling

To recover the state of the atmosphere, a numerical mesoscale model—the WRF model is applied (namely Advanced Research WRF (WRF-ARW), v. 4.1.2) (Skamarock et al., 2019; WRF model, 2020). The WRF model, being free software with centralized support, is one of the most widely used tools for atmospheric modeling. The strategy of two nested domains is applied, with the center at the observation point (40.4715°, 44.1815°). The outer domain with dimensions of 2,700 × 1,800 km^2 (the discretization step is 3 km) completely covers the Black and Caspian seas, the Caucasus mountains, Asia Minor, and the Armenian and Iranian highlands. The inner domain with dimensions of 90 × 90 km^2 (the discretization step is 1 km) reproduces in detail the Aragats mountain (see Figure 1). The vertical coordinate in the inner domain is described by an irregular grid of 41 levels, the discretization step takes values from 50 m (near the ground) to 600 m (at the height of 20 km). WRF modeling parameters are given in Supporting Information.

The advantage of the WRF model is the possibility of using various parameterizations of microphysical processes. Microphysical schemes differ, in particular, in the number of types of liquid and solid water particles taken into account, as well as in the spatial resolution of the simulation. Solid hydrometeors are known to carry a significant portion of the charge in a cloud (Saunders, 2008). The sign of the charge on solid hydrometeors of different types varies. Therefore, it is important to take into account as many species of solid hydrometeors as possible. The consideration of convective events occurring near a mountain top requires the best possible spatial resolution. The Thompson parameterization (Thompson et al., 2008) is

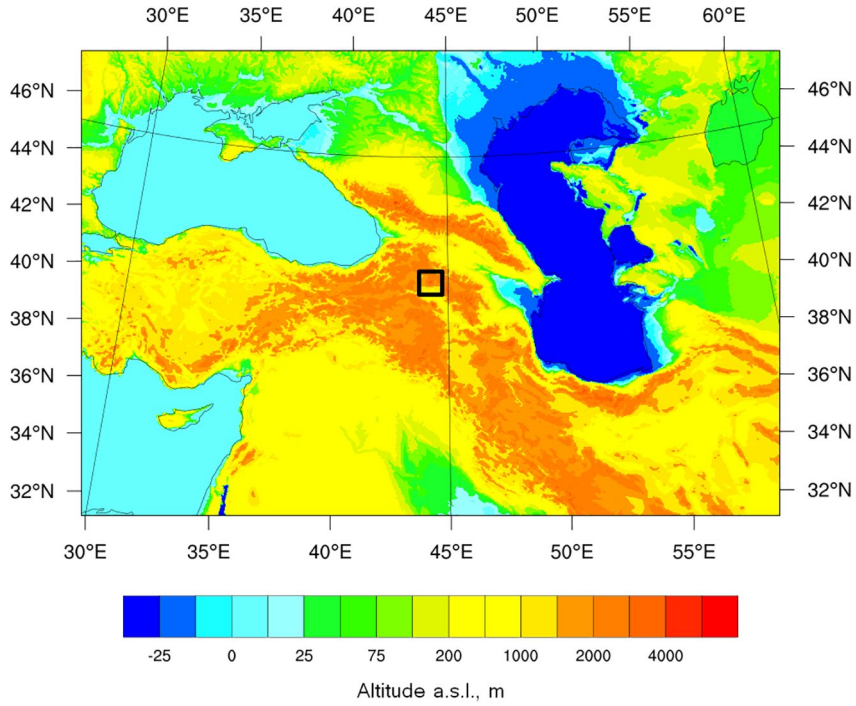

Figure 1. Modeling region, the outer and inner (black square) domains.

chosen for this study as optimal in terms of the number of described types of particles and the resolution. The Thompson-2008 scheme is recommended for calculations on fine meshes with the discretization step down to 1 km (WRF Model, 2019).

The applied parameterization of microphysical processes considers water vapor and five types of hydrometeors (snow particles, cloud ice particles, graupel particles, rain droplets, and cloud water droplets). Characteristic size ranges of hydrometeors are approximately the following: 0.001–1,000 μm for cloud ice, less than 10 mm for snow particles, less than 50 μm for cloud water droplets particles, more than 500 μm for rain droplets with a characteristic fall rate of 0.2–8 m/s (Thompson et al., 2008; Young, 1993). In agreement with generally accepted microphysical terms (Pruppacher & Klett, 2010, p. 40), in what follows, "ice" refers only to cloud ice (small solid water particles), although all solid hydrometeors (snow and graupel particles) consist of ice. The application of other widely used parameterizations with three or more solid hydrometeor types, namely WRF Double-Moment 6-class scheme (WDM6) and NSSL 2-moment scheme, showed us that the Thompson parameterization provides the best fit on a 1 km grid to the measurement data corresponding to convective events in the Aragats region. To take into account a realistic distribution of aerosols, an aerosol-aware microphysical parameterization by Thompson and Eidhammer (2014) was also applied, where the aerosol number concentrations were derived from multiyear global model simulations (Colarco et al., 2010). All aerosol particles within the parameterization are divided into two types: so-called ice-friendly aerosols (dust particles larger than 0.5 μm) and water-friendly aerosols (all other species). It should be noted that the simulated convective systems are mainly located above the zero isotherm, while the main processes associated with water-friendly aerosols occur at positive temperatures (Rosenfeld et al., 2008). The concentration of ice-friendly aerosols in the region under consideration was expected to be low, which is proved with the use of the aerosol-aware parameterization (see Supporting Information).

The initial 6–8 hours of the simulation, usually referred to as the "spin-up time," gives an unrepresentative simulation (Chu et al., 2018; Ulmer & Balss, 2016). The time interval during which the modeling is reliable starts just after the spin-up time and is 6–8 hours long. For this reason, the beginning of the simulation interval should be always chosen so that the event under investigation is after the spin-up. We use an additional condition: we consider only events with no clouds in the inner domain during the spin-up time (cloudiness is estimated by the measured surface electric field). This selection further improves the quality

of the modeling of convective systems. Additionally, it is known that geographic and climatic features have a significant impact on the rate of accumulation of modeling errors, while highly forced background conditions (in particular, mountainous terrain) can lead to an increase in the time interval of reliable modeling (Warner, 2011). Typically, the model was initialized 6–12 hours before the registered TGE and the simulation lasted for 12–24 hours, which leads to good reproduction of convective events. To initialize the WRF-ARW model, the data from the global data assimilation system GDAS based on the GFS model were used. The basic forecast error of the GFS model is estimated in White (2018) to be limited by 10%.

4. A Technique for Estimation of the Electric Charge Structure

To estimate the large-scale charge distribution within the cloud, we use the results of electric field measurements on the ground. The results of ground measurements of temperature and pressure are used for the verification of the modeling of the state of the atmosphere. A charge structure capable of producing the measured electric field dynamics is not unique; hence, the determination of the charge distribution requires additional assumptions. Data on charge separation processes derived from empirical studies are taken into account in the model, making it possible to uniquely determine the charge structure.

4.1. Assumptions on the Charge Distribution

From a mathematical point of view, the problem of determining the spatial charge distribution based on the surface value of the electric field is ill-posed. Strictly speaking, this problem has an infinite number of solutions. To select the most physically justified solution, it is necessary to make assumptions about the microphysical laws of charge distribution. The technique proposed here for the estimation of the cloud electrical structure using ground-based measurements is based on two main assumptions:

1. The electric field distribution is maintained by the charges of hydrometeors. The charge density for each type of solid hydrometeors (i.e., the charge on hydrometeors per unite volume) is considered to be proportional to the mass density of particles of this type (i.e., the mass of hydrometeors in a unit volume): $Q_j = \alpha_j m_j$, where Q_j is the charge density of hydrometeors of type j, α_j is a time-independent coefficient of proportionality, and m_j is the mass density for the particles of type j. The coefficients α_j are different for each hydrometeor type and each cloud: the value of α_j is defined by the intensity of electrification processes, which depends on the conditions in a cloud.
2. All energetic particle flux variations are due to changes in the electric field distribution (i.e., the variability of cosmic-ray flux is neglected).

The assumption of linear charge-mass dependence is based on the results of empirical studies (Takahashi, 1972; Takahashi et al., 1999). It is known that the maximal charge value on a graupel or snow particle corresponds to the middle part of the size distribution of these particles (Takahashi et al., 1999, Figure 16). In the framework of the chosen approach, charges on all other hydrometeors can be neglected (beyond the middle part of the size range), then approximately equal charges are located on all particles of approximately the same size and mass, which leads to proportionality between the mass density and the charge density. As the exact dependence of the charge on the particle type and size is unknown, the simplest model which would provide reasonable agreement with measurement results should be applied. The charge separation rate is approximately equal to the dissipation rate during the mature stage of a storm (McGorman & Rust, 1998, p. 33; Stolzenburg et al., 2015). Thus, to analyze a cloud at the mature stage, we consider a quasi-stationary mode with constant integral charge and mass of water particles. Dementyeva et al. (2015) showed the applicability of this approximation for the analysis of thunderclouds and lightning activity.

Thus, the particle flux at the Earth's surface is determined by the configuration of the electric field of the cloud, and the question of finding the charge distribution becomes equivalent to the question of finding the distribution of hydrometeors and the magnitudes of their charges. No simplifying assumptions about the geometry of the cloud structure are required. The recovery of the spatial distribution of the electric charge in the cloud is performed by comparing the measured and modeled dynamics of the vertical component of the electric field on the ground.

4.2. The Algorithm of Estimating the Charge Distribution

The estimation of the cloud electrical structure is carried out by the following sequence of actions:

1. For the TGE event under consideration, a time interval appropriate for modeling is determined. The main requirement is the absence of a significant surface electric field disturbance at the Station during the previous 6–8 hours, indicating the absence of electrified clouds.
2. For the chosen event and time interval the spatial distribution of hydrometeors (cloud ice particles, snow particles, graupel particles, rain droplets, and small water droplets) is recovered using WRF modeling, with a time step of 5 min, as described in the previous section. In what follows special attention is paid to the density of hydrometeors in the vicinity of the Station (the region of the main interest has a horizontal size of 6 km and the vertical size of 10 km, the horizontal discretization step is 1 km, and the vertical discretization step near the ground is about 50 m).
3. The charge density of hydrometeors of each type is assumed to follow their spatial distribution, so that for each node of the discretization grid the charge density follows the relation $Q_j = \alpha_j m_j$.
4. The dynamics of the surface electric field E_j induced by hydrometeors of type j at the observation point are calculated using the method of image charges in the approximation of a perfectly conducting surface. $E_j = \sum_i 2k\frac{Q_{ji}}{R_i^2}cos(\chi_i) = \alpha_j \sum_i 2k\frac{m_{ji}}{R_i^2}cos(\chi_i) = \alpha_j E_{0j}$, where k is the Coulomb constant, Q_{ji} and m_{ji} are the charge and mass of hydrometeors of type j simulated at the grid node number i, R_i is the distance between the grid node i and the point of observation, χ_i is the angle between the vertical and the direction from the grid node i to the point of observation. $E_{0j} = \sum_i 2k\frac{m_{ji}}{R_i^2}cos(\chi_i)$ is the surface electric field created by hydrometeors of type j under the assumption $\alpha_j = 1$. The resulting electric field at the observation point is $E = \sum_j E_j = \sum_j \alpha_j E_{0j}$.
5. The obtained time dependence of the electric field produced by hydrometeors of each type is compared with the time series of the measured electric field (both time series are averaged over 25 min to exclude the influence of the measured electric field variations associated with lightning discharges and the small-scale cloud structure, as well as inaccuracies of the simulation).

The set of the proportionality coefficients α_j providing the best fit of the measured surface electric field dynamics is determined by the linear regression procedure using the machine learning library (scikit-learn, 2020). The charge-mass coefficients for each event are assumed to be time-independent, so the optimization problem is defined as follows:

$$E_{measured}(t) = \sum_j \alpha_j E_{0j}(t), \tag{1}$$

where $E_{measured}(t)$ is the measured surface electric field (dependent on time), α_j is the charge-mass coefficient for the hydrometeor type "j" (summation is carried over hydrometeor types), and $E_{0j}(t)$ is the time-dependent surface electric field caused by hydrometeors of type "j" under the assumption of $\alpha_j = 1$.

The proposed technique of estimating the cloud electrical structure is based on the use of measurements of the surface electric field as the only characteristic of the charge distribution. Within the framework of the technique, the electric field dynamics are analyzed with 25-min averaging applied, enabling an estimate of the large-scale structure of a cloud. Thus, the technique is applicable for clouds with a sufficiently simple charge structure, which could be approximated by several charge regions. An event is considered suitable for applying the technique if sign reversals of the surface electric field during the event are infrequent (the time interval between two sign reversals should be 15 min or more). For the majority of the events, the electric field dynamics have one pronounced sign reversal, corresponding to a cloud with a dipole electrical structure, in which the centers of the charge layers are shifted relative to one another.

5. Analysis of TGE June 11, 2016

The algorithm presented in the previous section is illustrated by the procedure of estimating the electrical structure for the cloud that caused TGE events on June 11, 2016. A characteristic feature of the event is an intensification of the energetic particle flux, immediately following a rapid decrease of the electric field; this is in agreement with the fact that a negative electric field accelerates electrons toward the ground, and thus increases the energetic particle flux detected on the ground. Lightning strikes were not taken into account in the simulation because the resolution of WRF modeling significantly exceeds a time scale of lightning flashes. Thus, rapid changes of the electric field (10 kV/m and more per minute) are not reproduced in the modeling and are not related to a large-scale charge structure. In what follows, the numeration scheme corresponds to the description of the algorithm in the previous section.

1. An electric field variation accompanying the count rate disturbance was registered on the ground during the time interval from 10:40 to 12:10 UT. The initial point of WRF-modeling could be 00:00, 06:00, 12:00, or 18:00 UT. 6–8 hours of simulation preceding the considered electric field variation are required, which leads to the choice of 00:00 June 11, 2016, as the starting point for modeling (no electric field disturbance was registered during the first 8 hours of modeling, which implies the absence of electrified clouds above the Station.).
2. The distribution of cloud ice, snow, and graupel particles and liquid water particles is modeled for the period from 00:00 to 18:00 June 11, 2016. The dynamics of hydrometeor concentration, according to the modeling, are provided in Supporting Information.
3. The spatial charge distribution for each of the five kinds of hydrometeors (snow particles, cloud ice particles, graupel particles, rain droplets, and cloud water droplets) is estimated using the formula $Q_j = \alpha_j m_j$, where j denotes the type of hydrometeors. The coefficient α_j is to be found from modeling and measurement results.
4. The dynamics of the electric field E on the ground surface induced by hydrometeors of each type are calculated with the value of α_j assumed to be equal to 1. The dynamics of the electric field that could be created by charges on hydrometeors of each type are presented in Supporting Information.
5. The electric field on the ground created by hydrometeors of type j is assumed to be $\alpha_j \cdot E_{0j}$, where E_{0j} is the electric field on the ground found at the previous step under the assumption of $\alpha_j = 1$. The measured field dynamics are averaged over 25 min by the simple moving average method and compared with the simulated electric field dynamics. An optimization problem is solved. The set of α_j providing the best fitting of the measured electric field dynamics is determined by linear regression.

The impact of cloud ice on the surface electric field is found to be negligibly small, and for this reason $\alpha_{ice} = 0$ is assumed. Charge carriers are graupel and snow particles. The solution of the optimization problem for α_j can be interpreted as follows. In the time range 10:30–12:00 UT, the WRF shows the prevalence of graupel particles above the measurement location, and the measured surface electric field is positive. At 12:00–13:00 UT, the modeling shows that there are predominantly snow particles above the Station, and the measured surface electric field is negative. Therefore, graupel particles are charged positively, creating a positive surface electric field at 10:30–12:00 UT, and snow particles are charged negatively. The resulting modeled dynamics of the electric field are compared with the measured dynamics of the electric field on the ground (Figure 2a). Charges, and, consequently, electric fields of ice, rain, and cloud particles are found to be negligible.

The analysis described above leads to the conclusion that the cloud which caused the TGE of June 22, 2016 is characterized by a two-layer charge structure with the lower positive charge formed by graupel particles and the upper negative layer consisting of snow particles (Figures 2f and 2g). The distribution of graupel and snow particles above the Station at 11:20 UT is shown in Figures 2b and 2c. It could be seen that the graupel cluster is located below the snow cluster and is more localized (the horizontal size is about 3 km). The surface electric field at 11:20 UT is formed by a low dense cluster of positively charged graupel particles and a high negatively charged snow cluster; the resulting field (modeled and measured) is positive (Figure 2a). Negative surface field at 11:45 UT is formed mainly by the snow cluster which is more dense than the graupel cluster (Figures 2d and 2e).

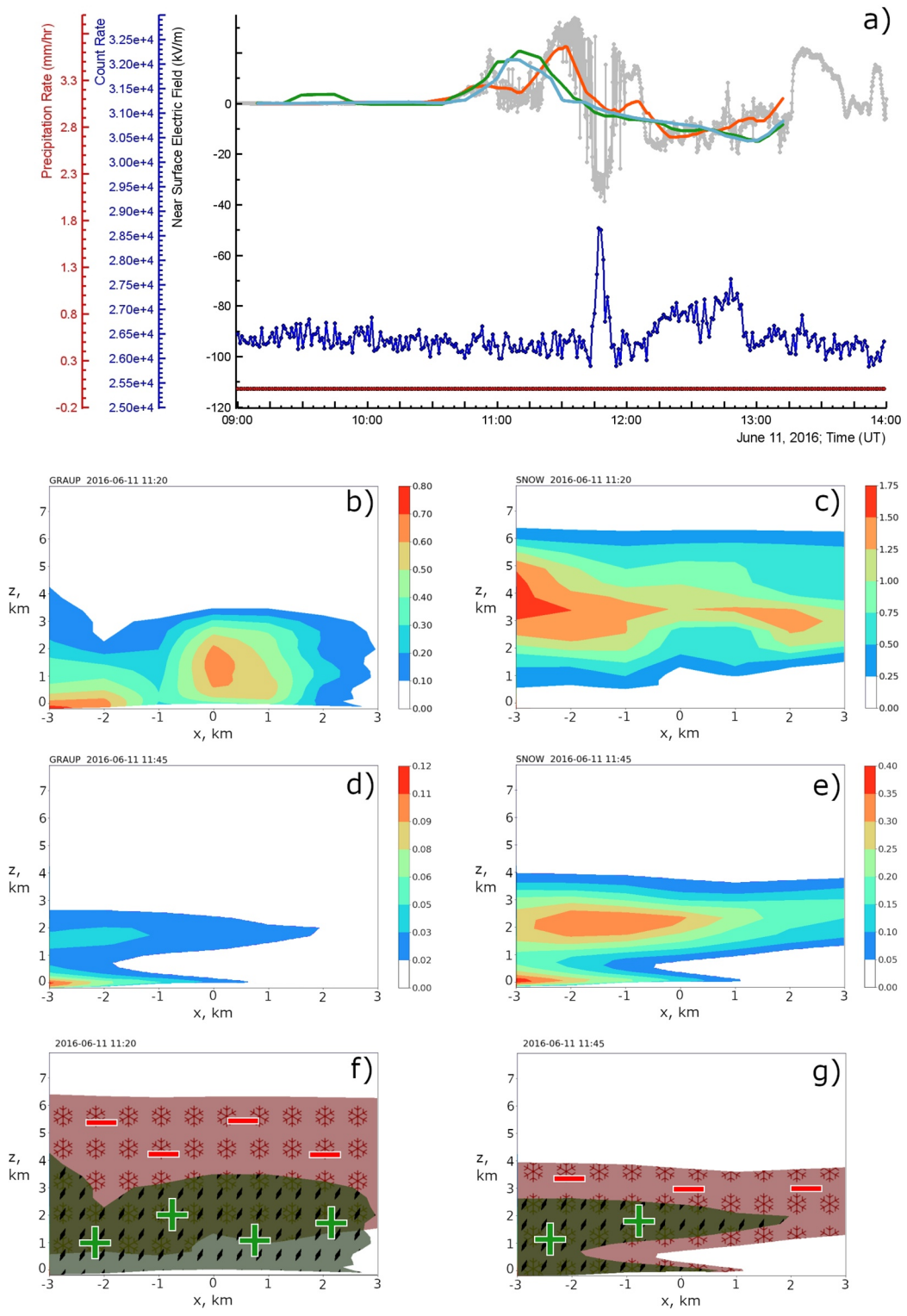

Figure 2. Analysis of TGE June 11, 2016: (a) the measured surface electric field (1-s series, gray curve), the energetic particle flux (excess over background values, 1-min series, blue curve), precipitation rate (red curve), the measured surface electric field averaged over 25 min (orange curve), the simulated surface electric field averaged over 25 min (green and cyan curves represent the electric field generated by the electric charges of snow and graupel particles simulated using Thompson-2008 and Thompson-2014 (aerosol-aware) parameterizations, respectively), (b, c) and (d, e) the modeled spatial distribution of the graupel and snow particles at 11:20 UT and 11:45 UT, respectively (the vertical plane contains the Station and is oriented from west to east, the coordinate origin corresponding to the location of the Station, the coloring of the regions characterizes the density in g/m^3), (f) and (g) the modeled electrical structure of the cloud at 11:20 and 11:45 UT, respectively, the snow cluster is red and the graupel cluster is green.

Figure 2a shows the comparison of the modeled and measured dynamics of the surface electric field. The surface electric field is reproduced on a time scale of about 20 min, which corresponds to the horizontal scale of about 2 km. A short-term disturbance of the electric field accompanying a TGE (11:45–11:55 UT) is not directly reflected by the averaged field dynamics and is not described by the developed model of a large-scale field structure, Figure 2a. Meanwhile, during the long-term enhancement of the energetic particles flux (12:00–13:00 UT), the electric field is negative, which is reproduced in the modeling. A configuration of the electric field with a negative value near the surface is known to be favorable for a TGE development. Thus, the developed model described large-scale features of electrical structure which leads to the creation of the TGE. Modeling results obtained using both microphysical schemes are in agreement with measurement data. Taking into account the aerosols in the parameterization of aerosols do not lead to significant changes in modeling results, which is consistent with the fact of a low concentration of aerosol particles in the modeled region (details on the distribution of aerosol particles are provided in Supporting Information).

The electric charge density per unit mass is estimated as 0.01 nC/m^3 for graupel and -0.02 nC/m^3 for snow. The integral electric charge in the column with a radius of 1 km above the Station: 0.1 C on graupel particles and −0.2 C on snow particles. The obtained values of charge density are of the same order of magnitude as the values typical for lightning-producing clouds (Rakov & Uman, 2004), and, therefore, are likely to form an electric field distribution favorable for avalanche multiplication of energetic particles. The applied technique of recovery of the cloud electrical structure allows for a more precise estimation of the charge of the lower charge layer because it is closer to the point of measurement.

A remarkable feature of the modeling result is that the relatively rapid decrease of the averaged electric field which occurred at about 11:45 UT, corresponds to the departure of the graupel cluster from above the Station, and the remaining cluster of snow particles induces a negative electric field (Figure 2a). Thus, the modeling provides a qualitative interpretation of the observed dynamics of the surface electric field, allowing us to see a correspondence between patterns of the electric field and types of charge carriers. The measured electric field variation starting at 13:30 UT is not described by our modeling and is not of interest for the consideration of the TGE phenomenon. In the simulation problem, the uncertainty is partially caused by the error in the initial conditions. The problem of the discrepancy between the simulation results and the measurements after the spin-up time has two reasons: the error of the initial data and the accumulation of errors of modeling, presumably mainly due to the microphysical scheme (we see that the main changes with time occur in the microphysics). To achieve better accuracy, techniques of assimilation of radar data should be applied. Our modeling showed that for the conditions of interest, the time interval for reliable simulation on a 1-km horizontal grid could not be longer than 8 hours.

6. Analysis of TGE June 21, 2017

In this section, a TGE event with a lower magnitude of the count rate increase is described. The steps of the electrical structure estimation are similar to those mentioned in the previous section. Here, the results of applying the technique to the event on June 21, 2017 are presented. The TGE of June 21, 2017 demonstrates a count rate increase at 21:15–21:25 UT shown in Figure 3a. A detailed analysis of the event is presented in Supporting Information.

Comparison of the modeled electric field dynamics with the measurement results is presented in Figure 3e. As for the event discussed in the previous section, the first positive and first negative electric field variations are described reasonably well, simulations of the electrical field using either of the microphysical schemes were equally successful. The electric field dynamics after 21:40 could not be modeled because of the limitations on the time interval of reliable modeling. The TGE of June 21, 2017 is accompanied by precipitation, which is typical of TGEs. Further research is needed for clarification of the relation between the rain rate and the surface dynamics of the electric field.

Figures 3b and 3c present the two-layered spatial structure of the cloud at 21:10 UT: graupel particles are located low above the ground surface, 2 km below the snow cluster. The movement of the lower clusters formed by graupel particles is correlated with the surface electric field variation of positive polarity, proving that the lower graupel cluster plays the role of the lower positive charge region in the formation of the electrical structure of a TGE-producing cloud. The vertical distance between the two charge clusters is about

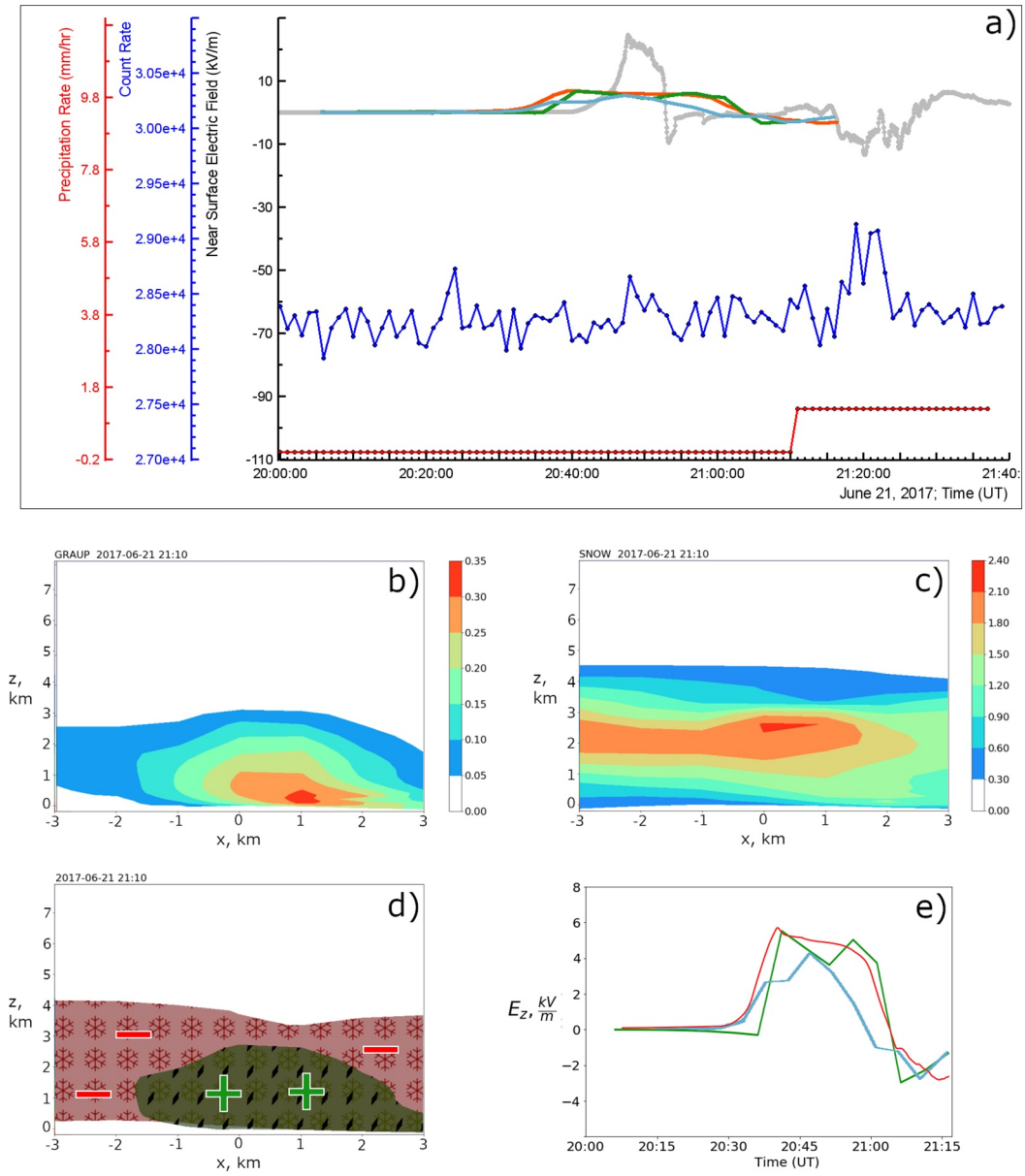

Figure 3. Analysis of TGE June 21, 2017, 20:30–21:05 UT: (a) the measured surface electric field (1- s series, gray curve), the energetic particle flux (excess over background values, 1-min series, blue curve), precipitation rate (red curve), the measured surface electric field averaged over 25 min (orange curve), the simulated surface electric field averaged over 25 min (green and cyan curves represent the electric field generated by the electric charges of snow and graupel particles simulated using Thompson-2008 and Thompson-2014 (aerosol-aware) parameterizations, respectively), (b, c) the modeled spatial distribution of the graupel and snow at 21:10 UT (zero horizontal and vertical coordinate values represent the location of the Station; the coloring of the regions characterizes the density in g/m^3), (d) the modeled electrical structure of the cloud at 21:10 UT, (e) enlarged fragment of (a)—averaged dynamics of surface electric field, measured and modeled.

Table 1
Parameters of the Modeled Charge Structures for TGE Events of 2016–2017

Date	Time	Count rate excess	Lower layer width, km	Upper layer width, km	Graupel density mg/m^3	Snow density mg/m^3	Positive charge density, nC/m^3	Negative charge density, nC/m^3
2016-05-04	19:05	1.12	5	5	800	1,500	0.050	0.020
2016-05-12	13:45	1.16	5	4	150	1,300	0.030	0.060
2016-06-08	11:40	1.17	1	4	120	2,000	0.020	0.025
2016-06-11	11:20	1.10	2	7	600	400	0.012	0.020
2017-06-21	21:10	1.03	3	5	250	2,000	0.017	0.026
2017-08-17	18:55	1.12	3	3	180	1,200	0.002	0.001
2017-10-01	18:05	1.05	3	4	150	1,000	0.002	0.005
2017-10-10	14:05	1.18	4	5	80	1,200	0.001	0.003

Note. For each event, the count rate excess (the relative enhancement of the count rate over the background), geometrical and electrical parameters of the modeled cloud structure are specified (the width, mass density, and charge density of the lower graupel cluster and the upper snow cluster).

2 km. The electric charge density per unit volume is estimated as (0.02 nC/m^3) for the graupel cluster and (−0.03 nC/m^3) for the snow cluster.

7. Modeling of TGE Events of 2016–2017 Seasons

Twenty-three TGE events with the energetic particle flux exceeding the background value by more than 10% were observed at the Aragats Research Station during 2016–2017. Eight events met the requirements listed in the previous section and were analyzed based on WRF-modeling. For all eight events, the estimated electrical structure is "an inverted dipole," where the upper negative charge cluster is formed by snow particles and the lower positive charge cluster—is formed by graupel particles. The cloud ice cluster and snow cluster are usually localized in the same region in the horizontal plane (the ice cluster could be 1–2 km above the snow cluster). However, the cluster of cloud ice is typically characterized by a much lower density and higher altitude than the snow cluster, from which it follows that the impact of cloud ice particles on the surface electric field is negligible. Characteristic values of the mass density for the two fractions are 0.4–2 g/m^3 for snow and 0.1–0.8 g/m^3 for graupel. The main parameters of the events and the corresponding charge structures are presented in Table 1. The size of the lower positive charge region is comparable with the size of the higher negative charge layer. The average width of the lower layer is 4 km, and the vertical size is 1.7 km. The average horizontal and vertical sizes of the upper charge layer are 5 and 2.7 km, respectively.

The charge per unit mass α for graupel and snow clusters typical for TGE producing clouds is found to be about 0.001–1 μC/kg (α values are provided in Supporting Information). The error of determination of the coefficient α is estimated as 20% and is related to the error of hydrometeor density estimation, which for typical parameters leads to the error in total charge of each layer about 0.02 C. The estimated values of the charge density are in agreement with the results previously found for cold cloud electrification: the analysis of charges on cloud ice and graupel particles in Hokuriku winter cumulus clouds (Takahashi et al., 1999) describes hydrometeors with a typical size of about 1 mm and the charge of 0.1–200 pC, which leads to the value of α of about 0.01–10 μC/kg. A charge density of 0.1 nC/m^3 in an inverted polarity storm is reported in Xu et al. (2016), which is close to the values found in Takahashi et al. (1999) and the present study. The characteristic electric charge density corresponds to the value of the cloud layer charge of about 0.1 C, which is lower than that for charge layers in mature thunderstorms (Rakov & Uman, 2004, p. 67). TGE is rarely observed in thunderclouds with intense lightning activity, which gives evidence of moderate charge values in TGE producing clouds.

8. Discussion and Conclusions

The WRF model was applied for the simulation of the state of the atmosphere during TGEs. The large-scale electrical structure of a cloud was modeled corresponding to the measured surface electric field dynamics. The majority of the considered events of the electric field and particle flux disturbances are caused by clouds with a dipole structure. The lower positive charged layer is formed by graupel particles, the higher negative layer consists of snow particles. The horizontal size of the lower positive charge usually lies in the range of 3–5 km, being comparable to the size of the negative charge layer. Additional evidence for the significance of the lower positive charge can be derived from statistics of lightning flashes in TGE-producing clouds: lightning flashes associated with the lower positive charge (inverted polarity IC) are shown to be more frequent than on average (Chilingarian et al., 2015; Chilingarian, Khanikyants, et al., 2019). It should be noted that the lower dipole plays a significant role in the initiation of the TGEs and lightning flashes on Aragats as well as on the Tibetan plateau. In Qie et al. (2005, 2015), it was established that larger than usual, the lower positive charge prevents negative cloud-to-ground lightning flashes (-CG) to occur, and only in the late stage of the storm–CG discharges could be triggered frequently. Nag and Rakov (2009) examined various scenarios of atmospheric discharges depending on the maturity of the lower positive charge. In Liu et al. (2013), it was stated that negative CG usually started as an inverted-polarity intracloud discharge which partly neutralized the lower positive charge so that a hole in the lower positive charge was formed and eventually led to a negative CG. In turn, the intense TGE can provide enough ionization to facilitate intracloud discharge, and usually discharges occurred just after the maximum of particle flux (Chilingarian et al., 2017). Based on the analysis of the TGE events abruptly terminated by lightning flash, Tsuchiya et al. (2011) provided firm evidence that the electric field between the main negative and lower positive charge regions in the thundercloud can be responsible for the flux enhancements at ground level TGEs can be abruptly terminated by inverted ICs occurring between the main negative charge region and the lower positive charge and by hybrid flashes (an inverted IC followed by a -CG). Thus, the conditions for electron acceleration toward ground needed for the production of TGEs consist in the creation of a strong electric field between the main negative charge region and the lower positive charge region.

It should be mentioned that there are two components of the upward electric field in the lower part of the cloud. One component is the electric field of a dipole formed by the main negative layer and mirror image charge, and the other is created by the lower positive charge. The performed analysis shows a definite correlation between the dynamics of the positively charged graupel cluster and the electric field time series, leading us to the conclusion that the lower positive charge is significant. The increase in the count rate took place simultaneously with the appearance of the lower positive charge above the Station, which points out that the field component related to the lower positive charge is important not only for the surface electric field but for the strong field region within the cloud as well, creating favorable conditions for TGE initiation.

The WRF simulation shows a very low density of hydrometers above the measurement point in the final time interval, while measurements show a nonzero near-surface electric field for the same time, indicating a presence of a significant amount of hydrometeors. We explain this by underestimation of the mass density of hydrometeors in the final parts of the simulation. The effect can be caused by the preceding overestimation of the precipitation density, which leads to a decrease in the water content of the modeled clouds. The underestimation of heavy rainfalls is known (Chu et al., 2018; Davitashvili et al., 2016; Gevorgyan, 2018; Kizhner et al., 2013; Kryza et al., 2013) and possibly has a similar origin as the overestimation of light precipitations observed in the present study (related to an oversimplified description of precipitation in the modeling system). The underestimation of the density of hydrometeors at the end of the modeling may be associated with the accumulation of errors mainly in the microphysical scheme, which can lead to a discrepancy with the radar data and requires the use of assimilation techniques.

We believe that one of the main directions of future study is the joint detailed analysis of radar data and modeling. An inspiring example of the analysis of the radar data together with electrical measurements helping to describe the structure of a cloud can be found in Williams et al. (1992). Nowadays, the errors of radar data and modeling make it possible to characterize the cloud structure with an accuracy of about 1 km. Improvements in computational methods and radar technology can lead to a decrease in error, which will confirm or deny the conclusions drawn here. Using the Thompson Aerosol Aware scheme, the realistic aerosol distribution is included in the modeling. However, more subtle effects of aerosols require a separate

study, combined with data assimilation. The developed model is a necessary step toward the analysis of convective events on the scale of TGE occurrence. Further development of modeling, including the application of techniques of radar data assimilation, may lead to the creation of a model of TGE-related charge distribution on a fine mesh. The presented description of a large-scale cloud structure is essential for simulation on smaller scales and can provide initial and boundary conditions for it. The proposed technique, in comparison with the explicit calculation of the distribution of electric charges using the WRF-ELEC (Fierro et al., 2013; Mansell et al., 2005; https://sourceforge.net/projects/wrfelec), has lower computational complexity. In addition, the results of the application of the technique allow for simpler interpretation of the charge structure, leading to a better understanding of electrification processes and conditions of development of electron avalanches, which cause TGE.

The influence of climatic conditions on the emission of gamma-rays by thunderclouds requires further research. Few studies of gamma-ray enhancements under electrified clouds in the mountains have been carried out so far. It is important to take into account Yair et al. (2019) and Reuveni et al. (2017), which report the gamma-ray enhancements measured at 2020 m above sea level (Mountain Hermon), most similar to the TGE observed in Aragats. Yair et al. (2019) describe the observation of the excess of gamma radiation over the background during a snow storm. Based on the analysis of the dynamics of the surface electric field strength, it is concluded that the snow particles carry a negative charge. (Reuveni et al. (2017) emphasize the role of the lower positive charge for the development of gamma-ray enhancements.

The performed analysis is important for obtaining new information about the cloud electrical structure and the processes of electrification that contribute to its formation, as well as for studying the TGE phenomenon. The characteristic vertical size of the region of the upward electric field in a typical cloud producing TGE is found to be 1–3 km, which is sufficient for the formation of energetic particle avalanches (Dwyer, 2003). Characteristic features of the time evolution of the energetic particle flux are explained by the modeled dynamics of the cloud electrical structure; a detailed consideration of the properties of TGEs and their origin remains the subject of further research.

Data Availability Statement

Measurement data is obtained at the Aragats Research Station and available at http://crd.yerphi.am/adei. The WRF-ARW model is available at http://www2.mmm.ucar.edu/wrf/users/downloads.html. WWLLN data can be obtained through http://wwlln.net.

Acknowledgments
The authors would like to thank H. Mkrtchyan and S. Hovakimyan for providing radar data, and all the reviewers for fruitful discussions.
Study on the numerical modeling was supported by a grant from the Government of the Russian Federation (Contract no. 075-15-2019-1892). Study on the analysis and interpretation of the results was supported by the Russian Science Foundation (Project no. 19-17-00218).

References

Chilingarian, A., Chilingarian, S., Karapetyan, T., Kozliner, L., Khanikyants, Y., Hovsepyan, G., et al.(2017). On the initiation of lightning in thunderclouds. *Scientific Reports*, *7*, 1371. https://doi.org/10.1038/s41598-017-01288-0

Chilingarian, A., Daryan, A., Arakelyan, K., Hovhannisyan, A., Mailyan, D., Melkumyan, L., et al.(2010). Ground-based observations of thunderstorm-correlated fluxes of high-energy electrons, gamma rays, and neutrons. *Physical Review D*, *86*, 072003.

Chilingarian, A., Hovsepyan, G., Elbekian, A., Karapetyan, T., Kozliner, L., Martoian, H., & Sargsyan, B. (2019). Origin of enhanced gamma radiation in thunderclouds. *Physical Review Research*, *1*. https://doi.org/10.1103/physrevresearch.1.033167

Chilingarian, A., Hovsepyan, G., Khanikyanc, G., Reymers, A., & Soghomonyan, S. (2015). Lightning origination and thunderstorm ground enhancements terminated by the lightning flash. *Europhysics Letters*, *110*, 49001328. https://doi.org/10.1209/0295-5075/110/49001

Chilingarian, A., Karapetan, T., & Melkumyan, L. (2013). Statistical analysis of the thunderstorm ground enhancements (TGEs) detected on Mt. Aragats. *Journal Advances in Space Research*, *52*(1178), 319. https://doi.org/10.1016/j.asr.2013.06.004

Chilingarian, A., Khanikyants, Y., Rakov, V. A., & Soghomonyan, S. (2020). Termination of thunderstorm-related bursts of energetic radiation and particles by inverted intracloud and hybrid lightning discharges. *Atmospheric Research*, *233*, 104713. https://doi.org/10.1016/j.atmosres.2019.104713

Chu, Q., Xu, Z., Chen, Y., & Han, D. (2018). Evaluation of the ability of the Weather Research and Forecasting model to reproduce a sub-daily extreme rainfall event in Beijing, China using different domain configurations and spin-up times. *Hydrology and Earth System Sciences*, *22*, 3391–3407. https://doi.org/10.5194/hess-22-3391-2018

Colarco, P., Da Silva, A., Chin, M., & Diehl, T. (2010). Online simulations of global aerosol distributions in the NASA GEOS-4 model and comparisons to satellite and ground-based aerosol optical depth. *Journal of Geophysical Research*, *115*. https://doi.org/10.1029/2009JD012820

Davitashvili, T., Kutaladze, N., Kvatadze, R., Mikuchadze, G., Modebadze, Z., & Samkharadze, I. (2016). Precipitations prediction by different physics of WRF model. *International Journal of Environmental Science*, *1*.

Dementyeva, S. O., Ilin, N. V., & Mareev, E. A. (2015). Calculation of the lightning potential index and electric field in numerical weather prediction models. *Izvestiya, Atmospheric and Oceanic Physics*, *51*, 186–192. https://doi.org/10.1134/s0001433815010028

Dwyer, J. (2003). A fundamental limit on electric field in air. *Journal of Geophysical Research*, *30*(20), 2055. https://doi.org/10.1029/2003gl017781

Efm-100 atmospheric electric field monitor. (2016). *Installation/operators guide for model efm-100c*. Retrieved from https://www.boltek.com/EFM-100C_Manual_121415.pdf

Fierro, A. O., Mansell, E. R., MacGorman, D. R., & Ziegler, C. L. (2013). The implementation of an explicit charging and discharge lightning scheme within the WRF-ARW model: Benchmark simulations of a continental squall line, a tropical cyclone, and a winter storm. *Monthly Weather Review*, *141*(07), 2390–2415. https://doi.org/10.1175/MWR-D-12-00278.1

Gevorgyan, A. (2018). Convection-permitting simulation of a heavy rainfall event in Armenia using the WRF model. *Journal of Geophysical Research*, *123*(19), 11008–11029. https://doi.org/10.1029/2017jd028247

Gurevich, A. V., Milikh, G. M., & Roussel-Dupré, R. (1992). Runaway electron mechanism of air breakdown and preconditioning during a thunderstorm. *Physics Letters A*, *165*, 463–468. https://doi.org/10.1016/0375-9601(92)90348-p

Kizhner, L., Bart, A., & Nahtigalova, D. (2013). Using the numerical WRF model for the prediction of weather parameters in Tomsk region. *BioClimLand*, (1), 29–35.

Kryza, M., Werner, M., Wałszek, K., & Dore, A. J. (2013). Application and evaluation of the WRF model for high-resolution forecasting of rainfall – A case study of SW Poland. *Metz*, *22*(5), 595–601. https://doi.org/10.1127/0941-2948/2013/0444

Liu, D., Qie, X., Pan, L., & Peng, L. (2013). Some characteristics of lightning activity and radiation source distribution in a squall line over north china. *Atmospheric Research*, *132–133*, 423–433. https://doi.org/10.1016/j.atmosres.2013.06.010

Lynn, B., & Yair, Y. (2010). Prediction of lightning flash density with the WRF model. *Advances in Geosciences*, *23*, 11–16. https://doi.org/10.5194/adgeo-23-11-2010

Mansell, E. R., Macgorman, D., Ziegler, C., & Straka, J. (2005). Charge structure and lightning sensitivity in a simulated multicell thunderstorm. *Journal of Geophysical Research*, *110*. https://doi.org/10.1029/2004JD005287

McGorman, D., & Rust, W. (1998). *The electrical nature of storms*. Oxford University Press.

Nag, A., & Rakov, V. A. (2009). Some inferences on the role of lower positive charge region in facilitating different types of lightning. *Geophysical Research Letters*, *36*. https://doi.org/10.1029/2008GL036783

Pruppacher, H., & Klett, J. (2010). *Microphysics of clouds and precipitation, second revised and expanded edition with an introduction to cloud chemistry and cloud electricity*.

Qie, X., Zhang, T., Chen, C., Zhang, G., Zhang, T., & Wei, W. (2005). The lower positive charge center and its effect on lightning discharges on the tibetan plateau. *Geophysical Research Letters*, *32*. https://doi.org/10.1029/2004GL022162

Qie, X., Zhang, Y., Yuan, T., Zhang, Q., Zhang, T., Zhu, B., et al. (2015). A review of atmospheric electricity research in china. *Advances in Atmospheric Sciences*, *32*, 169. https://doi.org/10.1007/s00376-014-0003-z

Rakov, V., & Uman, M. (2004). *Lightning: Physics and effects*.

Reuveni, Y., Yair, Y., Price, C., & Steinitz, G. (2017). Ground level gamma-ray and electric field enhancements during disturbed weather: Combined signatures from convective clouds, lightning and rain. *Atmospheric Research*, *196*, 142–150. https://doi.org/10.1016/j.atmosres.2017.06.012

Rosenfeld, D., Lohmann, U., Raga, G. B., O'Dowd, C. D., Kulmala, M., Fuzzi, S., et al. (2008). Flood or drought: How do aerosols affect precipitation?. *Science*, *321*, 1309. https://doi.org/10.1126/science.1160606

Saunders, C. (2008). Charge separation mechanisms in clouds. *Space Science Reviews*, *137*, 335–353. https://doi.org/10.1007/s11214-008-9345-0

scikit-learn. (2020). Retrieved from https://scikit-learn.org/stable/

Skamarock, W. C., Klemp, J. B., Dudhia, J., Gill, D. O., Liu, Z., Berner, J., et al. (2019). *A description of the advanced research WRF model version 4*. Retrieved from http://dx.doi.org/10.5065/1dfh-6p97

Stolzenburg, M., Marshall, T., & Krehbiel, P. (2015). Initial electrification to the first lightning flash in New Mexico thunderstorms. *Journal of Geophysical Research - D: Atmospheres*, *120*(11), 253–276. https://doi.org/10.1002/2015jd023988

Takahashi, T. (1972). Electric charge of small particles (1-40 μ). *Journal of the Atmospheric Sciences*, *29*, 921–928. https://doi.org/10.1175/1520-0469(1972)029<0921:ecosp>2.0.co;2

Takahashi, T., Tajiri, T., & Sonoi, Y. (1999). Charges on graupel and snow crystals and the electrical structure of winter thunderstorms. *Journal of the Atmospheric Sciences*, *56*, 1561–1578. https://doi.org/10.1175/1520-0469(1999)056<1561:cogasc>2.0.co;2

Thompson, G., & Eidhammer, T. (2014). A study of aerosol impacts on clouds and precipitation development in a large winter cyclone. *Journal of the Atmospheric Sciences*, *71*(10), 3636–3658. https://doi.org/10.1175/JAS-D-13-0305.1

Thompson, G., Field, P. R., Rasmussen, R. M., & Hall, W. D. (2008). Explicit forecasts of winter precipitation using an improved bulk microphysics scheme. Part II: Implementation of a new snow parameterization. *Monthly Weather Review*, *136*, 5095–5115. https://doi.org/10.1175/2008mwr2387.1

Thorpe, A. (2013). An evaluation of recent performance of ECMWF's forecasts. *Meteorology section of ECMWF Newsletter*, (137), 15–18.

Tsuchiya, H., Enoto, T., Yamada, S., Yuasa, T., Nakazawa, K., Kitaguchi, T., et al. (2011). Long-durationγray emissions from 2007 and 2008 winter thunderstorms. *Journal of Geophysical Research*, *116*. https://doi.org/10.1029/2010JD015161

Ulmer, F.-G., & Balss, U. (2016). Spin-up time research on the Weather Research and Forecasting model for atmospheric delay mitigations of electromagnetic waves. *Journal of Applied Remote Sensing*, *10*, 016027. https://doi.org/10.1117/1.JRS.10.016027

Warner, T. T. (2011). *Numerical weather and climate prediction*. Cambridge University Press.

White, G. (2018). *The development and success of NCEP's global forecast system*.

Williams, E. R., Geotis, S. G., Renno, N., Rutledge, S. A., Rasmussen, E., & Rickenbach, T. (1992). A radar and electrical study of tropical "hot towers". *Journal of the Atmospheric Sciences*, *49*, 1386–1395. https://doi.org/10.1175/1520-0469(1992)049⟨1386:ARAESO⟩2.0.CO;2 10.1175/1520-0469(1992)049<1386:araeso>2.0.co;2

Wrf model. (2019). *User's manual*. Retrieved from https://www.mmm.ucar.edu/weather-research-and-forecasting-model

Wrf model. (2020). Retrieved from https://www.mmm.ucar.edu/weather-research-and-forecasting-model

Xu, L., Zhang, Y., Liu, H., Zheng, D., & Wang, F. (2016). The role of dynamic transport in the formation of the inverted charge structure in a simulated hailstorm. *Science China Earth Sciences*, *59*, 1414–1426. https://doi.org/10.1007/s11430-016-5293-9

Yair, Y., Reuveni, Y., Katz, S., Price, C., & Yaniv, R. (2019). Strong electric fields observed during snow storms on Mt. Hermon, Israel. *Atmospheric Research*, *215*, 208–213. https://doi.org/10.1016/j.atmosres.2018.09.009

Young, K. (1993). *Microphysical processes in clouds*. Oxford University Press.